

Generating a Paracosm for Training-Free Zero-Shot Composed Image Retrieval

Tong Wang¹ Yunhan Zhao² Shu Kong^{1,3}

¹University of Macau ²Google DeepMind ³Institute of Collaborative Innovation

code: <https://github.com/leowangtong/Paracosm/>

Abstract

Composed Image Retrieval (CIR) is the task of retrieving a target image from a database using a multimodal query, which consists of a reference image and a modification text. The text specifies how to alter the reference image to form a “mental image”, based on which CIR should find the target image in the database. The fundamental challenge of CIR is that this “mental image” is not physically available and is only implicitly defined by the query. The contemporary literature pursues zero-shot methods and uses a Large Multimodal Model (LMM) to generate a textual description for a given multimodal query, and then employs a Vision-Language Model (VLM) for textual-visual matching to search the target image. In contrast, we address CIR from first principles by directly generating the “mental image” for more accurate matching. Particularly, we prompt an LMM to generate a “mental image” for a given multimodal query and propose to use this “mental image” to search for the target image. As the “mental image” has a synthetic-to-real domain gap with real images, we also generate a synthetic counterpart for each real image in the database to facilitate matching. In this sense, our method uses LMM to construct a “paracosm”, where it matches the multimodal query and database images. Hence, we call this method Paracosm. Notably, Paracosm is a training-free zero-shot CIR method. It significantly outperforms existing zero-shot methods on four challenging benchmarks, achieving state-of-the-art performance for zero-shot CIR.

1. Introduction

Composed Image Retrieval (CIR) formulates new scenarios in internet search [12] and e-commerce [39, 54], where it retrieves a target image from a database based on a user-provided multimodal query, which consists of a reference image and a modification text [51]. The text describes how to alter the reference image for which CIR algorithms should find the best matched image from the database [3, 29, 50].

Status Quo. CIR was addressed through supervised learning [6, 11, 14, 21, 30] over annotated triplets \langle reference image, modification text, target image \rangle . As curating large-

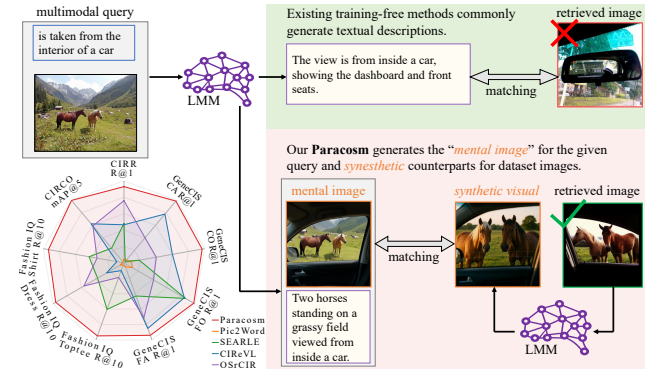


Figure 1. Overview of our method and benchmarking results. Unlike existing training-free methods [20, 44, 57] which use an LMM to generate descriptions for multimodal queries, we use it to generate “mental images” for the query and synthetic visuals for database images. Matching them effectively mitigates synthetic-to-real domain gaps and boosts CIR performance. Our final training-free zero-shot method *Paracosm* (Fig. 2) significantly outperforms existing zero-shot CIR methods, as summarized in the radar chart on standard benchmarks. See detailed results in Tables 1, 2 and 3.

scale triplet data is prohibitively expensive, recent works develop zero-shot CIR (ZS-CIR) approaches [7, 36, 44, 57]. Notably, ZS-CIR does not necessarily mean non-learning but emphasizes not directly training CIR models on data triplets. Rather, they still train models in an indirect way [16, 42, 43, 52, 59]. For example, many methods [7, 36] train textual inversion networks on image-text pairs to map images to text tokens for cross-modal matching; some [26, 52] synthesize a pseudo image for the multimodal query using pretrained image generative models [34, 37, 62] to assist with cross-modal matching. To contrast training-based ZS-CIR approaches, training-free methods [20, 44, 57] propose to exploit Large Multimodal Models (LMMs) [10, 32, 49] to generate a description for the multimodal query, and use it for text-to-image (T2I) matching for CIR.

Insights. The fundamental challenge of CIR is that the multimodal query only implicitly defines a “mental image”, which does not physically exist to be used for retrieving the corresponding target image. We aspire to address this challenge from first principles by generating a “mental image” for a given query to enable more accurate matching (Fig. 1).

While existing works have exploited LMMs to generate descriptions, we leverage LMMs for image generation based on multimodal queries [53]. Yet, as the generated “mental image” has synthetic-to-real domain gaps from the real images in the dataset, we propose to generate a synthetic counterpart for each dataset image, which is used to facilitate matching. As our method essentially uses LMMs to define a synthetic or virtual space, like a “paracosm”, we name our method **Paracosm**. Notably, *our Paracosm is a training-free zero-shot CIR method*. To validate Paracosm, we follow the established experiment protocols that use pretrained Vision-Language Models (VLMs) [18, 33] for matching. Extensive experiments on four challenging benchmarks demonstrate that Paracosm resoundingly outperforms existing ZS-CIR methods (ref. a summary in Fig. 1).

Contributions. We make three major contributions:

1. We solve CIR from first principles with the training-free method Paracosm. It generates “mental images” for multimodal queries to facilitate matching with dataset images.
2. We mitigate the synthetic-to-real domain gaps of mental images by generating synthetic counterparts for database images. Matching them together boosts CIR performance.
3. On four standard benchmarks, we demonstrate that Paracosm resoundingly outperforms existing CIR approaches, achieving state-of-the-art performance.

2. Related Work

Composed Image Retrieval (CIR) extends traditional retrieval tasks, such as text-to-image retrieval and image-to-image retrieval, by allowing users to use multimodal queries in retrieval [51]. CIR was initially approached by supervised learning methods [6, 11, 14, 21, 30], i.e., training models over annotated data triplets \langle reference image, modification text, target image \rangle . These methods [6, 17, 47, 55, 60, 61] propose to train a Transformer or an MLP atop pretrained backbones over the annotated data triplets, intending to fuse the reference image and the modification text in a feature space and to allow matching with dataset images. Some methods [22, 30, 31] finetune a pretrained Vision-Language Model (VLM) [23, 33] for better matching between multimodal queries and dataset images. However, as supervised learning methods require costly curation of triplet data, recent methods explore zero-shot CIR (ZS-CIR) [7, 16, 20, 26, 36, 44, 52, 57]. We explore *training-free* ZS-CIR and introduce a rather simple method that rivals some recent supervised methods.

Zero-Shot Composed Image Retrieval (ZS-CIR) aims to solve CIR without directly training on triplet data [36]. It does not mean developing training-free methods but allows training in an indirect manner [7, 16, 36, 42, 43, 59]. For

example, many methods train a textual inversion network on existing image datasets [35, 38], mapping the reference image to a pseudo-word token, which, along with the modification text, is used in cross-modal matching with dataset images. A couple of recent methods [26, 52] use pretrained generative models [34, 37, 62] to synthesize a synthetic image (similar to our “mental image”), termed as pseudo-target images, for a given multimodal query and use it to augment the textual feature (i.e., output by the textual inverse network) to compute similarity scores with dataset images. Importantly, training-free ZS-CIR methods [20, 44, 57] have emerged that leverage an LMM to generate a description for a given multimodal query. This avoids training a separate textual inversion network. Notably, existing ZS-CIR methods have not considered generating either descriptions or synthetic images for database images. In contrast, our work does so, motivated to address ZS-CIR from first principles. Specifically, we propose to generate the “mental image” for the query and synthetic counterparts for real dataset images, mitigating synthetic-to-real domain gaps for better performance.

Foundation Models (FMs), pretrained on various formats of web-scale data, demonstrate unprecedented performance on downstream tasks in a zero-shot manner. FMs are extensively exploited in the CIR literature [8, 9, 25, 28, 56]. First, Vision-Language Models (VLMs), pretrained on web-scale image-text pairs [18, 33], are commonly used in CIR to extract features of modification texts and images, enabling cross-modality matching [6, 20, 26, 44]. Second, Large Language Models (LLMs), pretrained on massive text corpus [4, 10, 41, 48], are used in CIR for generating a target image description by incorporating the reference image caption and the modification text [26, 57]. Third, Large Multimodal Models (LMMs) [5, 32, 45, 53], pretrained on web-scale multimodal data and typically larger than VLMs in parameter size, are used in CIR to generate image captions [20, 26, 57] for multimodal queries. Earlier CIR works use LMMs to create triplet data for supervised training [28, 43, 59]. Most training-free ZS-CIR methods [20, 44, 57] use LMMs to generate textual descriptions for multimodal queries and utilize a VLM to match the descriptions with database images, transforming the CIR task to a text-to-image retrieval problem. Following this literature, we extensively exploit LMMs to generate “mental images” for multimodal queries and synthetic counterparts for real database images. Matching them effectively mitigates synthetic-to-real domain gaps and boosts CIR performance.

3. Methodology

We begin by defining the ZS-CIR problem and its development protocol, then introduce our rather simple *training-free* method Paracosm. Fig. 2 previews its pipeline.

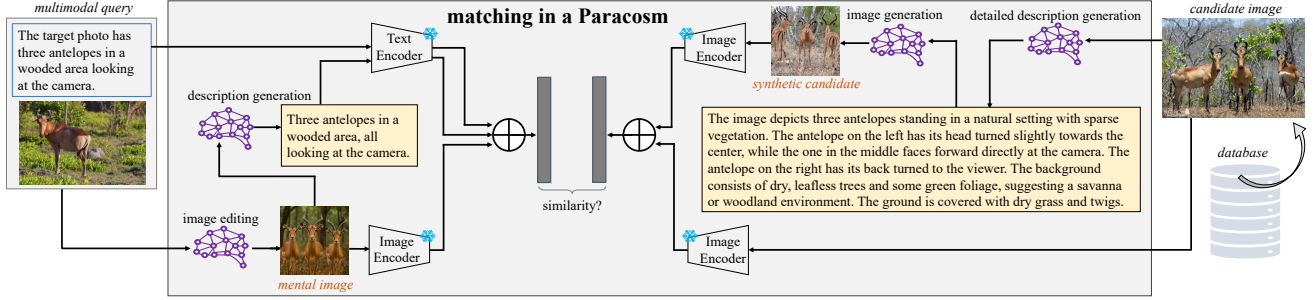


Figure 2. **Flowchart of our zero-shot training-free CIR method Paracosm.** Given a multimodal query that consists of a reference image and a modification text, we feed it to an LMM to generate a “mental image”. We further generate a brief description for it. Both the “mental image” and description, as well as the modification text, are used as feature representation for the query. As the “mental image” is synthetic, we mitigate synthetic-to-domain gaps by generating synthetic counterparts for dataset images. To do so, we use the LMM to generate *detailed* descriptions, which are used as prompts for image generation. Both the real and synthetic visuals are used as representations for database images. In plain language, our method uses LMMs to create a virtual paracosm, where it matches the query and dataset images.

3.1. Preliminaries of Zero-Shot CIR

Task Definition. Let $(\mathbf{I}_{ref}, \mathbf{t}_{mod})$ represent the reference image and modification text of a given multimodal query. \mathbf{t}_{mod} describes how to alter \mathbf{I}_{ref} to match what the user wants to search for, i.e., a target image \mathbf{I}_{target} from a given database consisting of n candidate images $\{\mathbf{I}^1, \mathbf{I}^2, \dots, \mathbf{I}^n\}$. ZS-CIR aims to develop methods to retrieve target images for multimodal queries, without directly training on annotated data triplets $(\mathbf{I}_{ref}, \mathbf{t}_{mod}, \mathbf{I}_{target})$.

Methodology Development. While ZS-CIR eschews a training set of annotated triplet data, it still allows exploiting data available in the open world and pretrained FMs therein. Following this protocol, existing ZS-CIR methods leverage LMMs in different ways, e.g., using a VLM for cross-modality matching [7, 16, 36] and an LMM to generate descriptions [20, 44, 57]. By exploiting open-world data [35, 38], some methods train necessary models for fusing \mathbf{I}_{ref} and \mathbf{t}_{mod} into features [7, 16, 36], or for generating pseudo images for the multimodal query [26, 52]. In this work, we aspire to develop a *training-free* method by extensively leveraging LMMs, without training any new models. Next, we present our method Paracosm in detail.

3.2. The Proposed Method: Paracosm

Paracosm is a rather simple method that processes multimodal queries and database images using LMMs. Below we describe how it processes them and match them for retrieval.

Processing Multimodal Query. For a multimodal query, Paracosm first generates the “mental image” \mathbf{I}_{mental} using an LMM [53]. Based on this mental image \mathbf{I}_{mental} , it further generates a brief description \mathbf{t}_{query} , which can be thought of as the description of the target image \mathbf{I}_{target} . Some recent methods [20, 44, 57] propose to generate such a description based on the multimodal query, e.g., by first generating a description for the reference image and then revising it with the modification using an LLM. Fig. 3 shows that solely relying on the generated description misses crucial visual

information, whereas the mental image keeps rich information and incorporating it boosts CIR. Table 5 quantitatively verifies this.

Processing Database Images. As the generated mental images are synthetic and have synthetic-to-real domain gaps, directly matching them with real images from the database is suboptimal. To mitigate this gap, Paracosm also generates a synthetic visual \mathbf{I}_{syn}^i for each database image \mathbf{I}^i . To this end, Paracosm first leverages an LMM [46], to generate a *detailed* description. It then uses this description as prompt to a text-to-image generation model [53], generating a synthetic counterpart for each database image. The real database images and synthetic counterparts are used jointly for matching a multimodal query. Table 5 validates this design choice.

Matching for Retrieval. After transforming both multimodal queries and database images into the virtual paracosm, we construct features using a pretrained VLM, which consists of a visual encoder $V(\cdot)$ and a text encoder $T(\cdot)$. Specifically, the query feature \mathbf{q} and the i^{th} database image feature ϕ^i are computed below:

$$\mathbf{q} = \lambda(V(\mathbf{I}_{mental}) + T(\mathbf{t}_{query})) + (1 - \lambda)T(\mathbf{t}_{mod}) \quad (1)$$

$$\phi^i = V(\mathbf{I}^i) + V(\mathbf{I}_{syn}^i)$$

where λ is a hyperparameter controlling the contribution of incorporating the modification text \mathbf{t}_{mod} . Finally, Paracosm computes the cosine similarity score and returns the index of the potential target image:

$$i^* = \operatorname{argmax}_{i=1 \dots n} \frac{\mathbf{q}^T \phi^i}{\|\mathbf{q}\|_2 \|\phi^i\|_2}$$

3.3. Remarks

Paracosm makes better use of LMMs. Existing ZS-CIR approaches [20, 44, 57] also leverage LMMs but focus on generating descriptions for multimodal queries and transforming the CIR problem into a text-to-image retrieval problem. However, text descriptions alone cannot sufficiently



Figure 3. **Comparison of qualitative results** between OSrCIR [44] and our Paracosm. We show four examples from the CIRCO dataset [3] in the first column, followed by generated descriptions and top-4 retrievals by OSrCIR, and the mental images and top-4 retrievals by Paracosm. For each multimodal query, OSrCIR uses an LMM to generate a description, uses it to match database images, and returns top ranked ones. Instead, Paracosm uses an LMM to generate a “mental image” for each query, which contains much richer information than a description, allowing image-to-image matching for better retrieval. Consequently, Paracosm yields better retrievals than OSrCIR.

capture rich visual information crucial to CIR and hence often lead to incorrect retrieved images, as demonstrated in Fig. 3. A couple of recent works [26, 52] realize the importance of incorporating pseudo-target images to facilitate CIR, e.g., by exploiting a pretrained text-to-image (T2I) generative model [62] to synthesize a pseudo-target image based on a description. Differently, we leverage an LMM that has image editing capability, i.e., editing the reference image based on the modification text into a “mental image”. As shown in Table 4, editing reference images yields better CIR results than T2I generation of pseudo-target images. Moreover, Paracosm exploits an LMM to generate detailed descriptions for each database image, and uses this description as prompt to generate a synthetic counterpart.

Is CIR still needed given the high-quality edited images? This question emerges in front of the high quality of the generated “mental images” based on multimodal queries (Fig. 3). We argue that CIR is still important in real-world visual search applications. For example, in e-commerce and fashion industry, users might want to base on a photo of clothes and search a different genre or style in an e-shop by specifying how to alter the photo. That said, no matter how photorealistic a mental image is, image generation cannot replace a real product in inventory.

Computation cost. As Paracosm extensively exploits LMMs, it has a high computation cost, especially for generating images, i.e., the mental images for the query and synthetic counterparts of database images. Yet, this is not a flaw pertaining only to Paracosm, as existing works also rely on generative models for retrieval. For example, prevailing ZS-CIR methods use LMMs to generate descriptions

[20, 26, 44, 57], and some turn to generative models to synthesize images [26, 52]. Importantly, like these methods, Paracosm can process database images ahead of time, and does not require computing features for them on the fly during inference. So the major computation overhead is on the process of a given multimodal query in inference, including generating the corresponding mental images and their descriptions. It is worth noting that efficient inference in generative models is an important topic and has been greatly advanced through model optimization [19, 58] and optimized implementation [15]. Therefore, Paracosm should not suffer from computation in the long run.

4. Experiments

We conduct extensive experiments to validate the proposed Paracosm, comparing it against existing methods and ablating its components. We start by datasets, metrics, implementation details, and compared methods.

Datasets. Following the literature [7, 16, 20, 36, 44, 52, 57], we use four established benchmarks, namely CIRR [29], CIRCO [3], Fashion IQ [54], and GeneCIS [50]. These datasets are publicly available for non-commercial research and educational purposes. CIRCO and GeneCIS are released under the CC-BY-NC 4.0 license; CIRR is licensed under CC-BY 4.0; Fashion-IQ is distributed under the Community Data License Agreement (CDLA). As we focus on ZS-CIR, we do not exploit their training data to develop models. For Fashion IQ, which only releases its validation set, we benchmark methods on this val-set; for other datasets, we benchmark methods on their official test sets. Moreover, Fashion IQ and GeneCIS have multiple subsets for testing, we report

Table 1. **Benchmarking results on CIRCO and CIRR test sets.** Our Paracosm resoundingly outperforms all the compared methods across different backbones and even rivals some recent supervised learned methods. Note that the recent method OSrCIR state in its paper that it used CLIP backbone but its open-source Github repository clarifies that it actually used OpenCLIP on CIRCO [2]. To comprehensively evaluate it, we copy the results from its paper (marked in red shade) and re-implement it using different backbones (marked in blue shade). Our reimplementations with OpenCLIP yield comparable results with what were reported in the paper of OSrCIR. Moreover, with OSrCIR, we compare using GPT-4o vs. Qwen2.5-VL to generate descriptions, finding that the former leads to better CIR results. Nevertheless, our Paracosm leverages the latter and still performs the best on the two benchmarks.

Backbone	Method	venue&year	CIRR							CIRCO			
			Recall@k				Recall _{Subset} @k			k=5	mAP@k		
			k=1	k=5	k=10	k=50	k=1	k=2	k=3		k=10	k=25	k=50
supervised methods	Combiner [6]	CVPR'22	33.59	65.35	77.35	95.21	62.39	81.81	92.02	–	–	–	–
	BLIP4CIR [30]	WACV'24	40.17	71.81	83.18	95.69	72.34	88.70	95.23	–	–	–	–
	CLIP-ProbCR [24]	ICMR'24	23.32	54.36	68.64	93.05	54.32	76.30	88.88	–	–	–	–
CLIP ViT-B/32	Image-only	baseline	6.89	22.99	33.68	59.23	21.04	41.04	60.31	1.34	1.60	2.12	2.41
	Text-only	baseline	21.81	45.22	57.42	81.01	62.24	81.13	90.70	2.56	2.67	2.98	3.18
	Image+Text	baseline	11.71	35.06	48.94	77.49	32.77	56.89	74.96	2.65	3.25	4.14	4.54
	SEARLE [7]	ICCV'23	24.00	53.42	66.82	89.78	54.89	76.60	88.19	9.35	9.94	11.13	11.84
	CIG + SEARLE [52]	CVPR'25	25.54	55.01	68.24	90.72	57.52	78.36	89.35	10.45	11.02	12.34	13.00
	LDRE [57]	SIGIR'24	25.69	55.13	69.04	89.90	60.53	80.65	90.70	17.96	18.32	20.21	21.11
	CIReVL [20]	ICLR'24	23.94	52.51	66.00	86.95	60.17	80.05	90.19	14.94	15.42	17.00	17.82
	OSrCIR [44] w/ GPT-4o	CVPR'25	25.42	54.54	68.19	–	62.31	80.86	91.13	18.04	19.17	20.94	21.85
	OSrCIR w/ GPT-4o	reproduced	25.81	54.34	67.61	89.45	61.01	80.27	90.29	14.91	15.34	16.79	17.60
	OSrCIR w/ Qwen2.5-VL	reproduced	23.35	51.42	64.29	86.24	57.16	76.41	87.52	11.84	12.39	13.53	14.27
	Paracosm	ours	32.27	62.60	75.16	92.60	65.16	83.25	92.34	26.10	27.02	29.29	30.45
CLIP ViT-L/14	Pic2Word [36]	CVPR'23	23.90	51.70	65.30	87.80	53.76	74.46	87.07	8.72	9.51	10.64	11.29
	SEARLE [7]	ICCV'23	24.24	52.48	66.29	88.84	53.76	75.01	88.19	11.68	12.73	14.33	15.12
	LinCIR [16]	CVPR'24	25.04	53.25	66.68	–	57.11	77.37	88.89	12.59	13.58	15.00	15.85
	CIG + SEARLE [52]	CVPR'25	26.72	55.52	68.10	89.59	57.95	77.81	89.45	12.84	13.64	15.32	16.17
	IP-CIR + LDRE [26]	CVPR'25	29.76	58.82	71.21	90.41	62.48	81.64	90.89	26.43	27.41	29.87	31.07
	LDRE [57]	SIGIR'24	26.53	55.57	67.54	88.50	60.43	80.31	89.90	23.35	24.03	26.44	27.50
	CIReVL [20]	ICLR'24	24.55	52.31	64.92	86.34	59.54	79.88	89.69	18.57	19.01	20.89	21.80
	OSrCIR [44] w/ GPT-4o	CVPR'25	29.45	57.68	69.86	–	62.12	81.92	91.10	23.87	25.33	27.84	28.97
	OSrCIR w/ GPT-4o	reproduced	26.51	55.88	68.77	88.17	61.69	80.29	89.88	17.70	18.56	20.52	21.47
	OSrCIR w/ Qwen2.5-VL	reproduced	22.77	51.88	63.59	85.74	57.21	76.65	88.05	14.06	14.93	16.65	17.50
	Paracosm	ours	31.95	61.56	72.96	92.00	64.68	82.89	91.47	30.24	31.51	34.29	35.42
OpenCLIP ViT-B/32	OSrCIR w/ GPT-4o	reproduced	32.96	63.28	74.99	92.29	66.72	84.39	93.08	18.77	19.33	21.04	22.02
	OSrCIR w/ Qwen2.5-VL	reproduced	29.18	58.43	70.27	89.69	62.17	80.58	90.46	14.47	15.23	16.70	17.55
	Paracosm	ours	36.29	68.29	79.74	94.34	69.52	85.78	94.07	31.31	32.48	35.19	36.33
OpenCLIP ViT-L/14	OSrCIR w/ GPT-4o	reproduced	35.47	65.06	76.96	92.99	67.42	85.66	93.30	22.75	23.51	25.73	26.78
	OSrCIR w/ Qwen2.5-VL	reproduced	31.59	61.06	72.60	90.84	63.35	81.86	90.82	17.88	18.72	20.51	21.39
	Paracosm	ours	38.24	68.80	78.84	94.72	70.60	85.90	93.78	37.40	38.64	41.57	42.73

results on each of them. We provide more details in the supplementary Section A.

Metrics. Following prior arts [16, 20, 44, 57], we use Recall@k (R@k) as the metric for CIRR, Fashion IQ and GeneCIS. For CIRCO, we use mean average precision (mAP@k) as it has more target images for queries.

Implementation Details. Following the literature [20, 44, 57], we report the results of all the methods by using CLIP ViT-B/32 and ViT-L/14 for matching. The LMMs used in Paracosm are Qwen2.5-VL-7B-Instruct [46], Qwen-Image [53], and Qwen-Image-Edit [53], for description generation, database image synthesis, and “mental image” generation. For fair comparison, especially with the state-of-the-art ZS-CIR method OSrCIS [44], we re-implement it and use GPT-4o for description generation (as done by OSrCIS). We run Qwen-Image-Edit on an NVIDIA A100 GPU as it requires more GPU memory [53]. Section B shows the detailed generation process. After generating “mental images” for multimodal queries, we use a single NVIDIA 4090

GPU for the remaining computation, e.g., extracting visual and textual features, generating descriptions and synthetic visuals for database images.

Compared Methods. We compare our Paracosm with representative and recent ZS-CIR methods, which can be categorized into training-dependent and training-free groups. We also compare baseline methods.

- *Baseline methods* include “image-only” which uses the feature of reference image for matching database images, “text-only” which uses modification text for cross-modality matching, and “image+text” which sums image and text features for matching.
- *Training-dependent methods* include Pic2Word [36], SEARLE [7], LinCIR [16], CIG [52] and IP-CIR [26]. All these methods rely on textual features, e.g., training a textual inverse network to map references images into pseudo-word tokens and merge them with textual tokens of modification texts. Notably, IP-CIR and CIG generate pseudo-target images for multimodal queries using a pre-

Table 2. **Benchmarking results on the Fashion IQ validation set.** Paracosm performs the best or second best across all backbones. Like in Table 1, we particularly study the recently published competitor OSrCIR with different backbones. Refer to Table 1 caption for conclusions.

Backbone	Method	venue&year	Shirt		Dress		Toptee		Average	
			R@10	R@50	R@10	R@50	R@10	R@50	R@10	R@50
supervised methods	Combiner [6]	CVPR'22	36.36	58.00	31.63	56.67	38.19	62.42	35.39	59.03
	PL4CIR [61]	SIGIR'22	33.22	59.99	46.17	68.79	46.46	73.84	41.98	67.54
	Uncertainty retrieval [13]	ICLR'24	32.61	61.34	33.23	62.55	41.40	72.51	35.75	65.47
CLIP ViT-B/32	Image-only	baseline	6.97	14.08	4.46	11.90	6.22	13.62	5.88	13.20
	Text-only	baseline	7.36	14.97	4.86	13.04	7.04	14.94	6.42	14.32
	Image+Text	baseline	12.46	24.88	11.90	28.85	15.45	29.27	13.27	27.67
	SEARLE [7]	ICCV'23	24.44	41.61	18.54	39.51	25.70	46.46	22.89	42.53
	CIG + SEARLE [52]	CVPR'25	24.73	41.46	18.94	39.66	25.50	46.66	23.06	42.59
	LDRE [57]	SIGIR'24	27.38	46.27	19.97	41.84	27.07	48.78	24.81	45.63
	CIReVL [20]	ICLR'24	28.36	47.84	25.29	46.36	31.21	53.85	28.29	49.35
	OSrCIR [44] w/ GPT-4o	CVPR'25	31.16	51.13	29.35	50.37	36.51	58.71	32.34	53.40
	OSrCIR w/ GPT-4o	reproduced	22.82	39.16	15.27	34.56	19.38	36.92	19.15	36.88
	OSrCIR w/ Qwen2.5-VL	reproduced	21.25	36.46	14.92	32.52	20.09	39.16	18.75	36.05
CLIP ViT-L/14	Paracosm	ours	29.20	46.91	20.82	41.94	28.40	50.33	26.14	46.39
	Pic2Word [36]	CVPR'23	26.20	43.60	20.00	40.20	27.90	47.40	24.70	43.70
	SEARLE [7]	ICCV'23	26.89	45.58	20.48	43.13	29.32	49.97	25.56	46.23
	LinCIR [16]	CVPR'24	29.10	46.81	20.92	42.44	28.81	50.18	26.28	46.49
	CIG + LinCIR [52]	CVPR'25	28.90	47.25	21.12	43.88	29.78	50.54	26.60	47.22
	LDRE [57]	SIGIR'24	31.04	51.22	22.93	46.76	31.57	53.64	28.51	50.54
	CIReVL [20]	ICLR'24	29.49	47.40	24.79	44.76	31.36	53.65	28.55	48.57
	OSrCIR [44] w/ GPT-4o	CVPR'25	33.17	52.03	29.70	51.81	36.92	59.27	33.26	54.37
	OSrCIR w/ GPT-4o	reproduced	25.76	42.49	18.39	37.58	24.89	44.11	23.01	41.39
	OSrCIR w/ Qwen2.5-VL	reproduced	23.85	39.94	15.96	35.89	23.05	42.63	20.95	39.49
OpenCLIP ViT-B/32	Paracosm	ours	31.55	49.51	22.91	45.61	31.82	52.83	28.76	49.32
	OSrCIR w/ GPT-4o	reproduced	31.26	51.08	28.36	48.98	34.63	56.71	31.41	52.26
	OSrCIR w/ Qwen2.5-VL	reproduced	27.97	47.25	23.15	44.62	28.51	50.18	26.54	47.35
OpenCLIP ViT-L/14	Paracosm	ours	36.70	54.51	29.40	51.66	39.32	61.96	35.14	56.04
	OSrCIR w/ GPT-4o	reproduced	31.40	50.74	28.61	49.43	34.63	55.53	31.55	51.90
	OSrCIR w/ Qwen2.5-VL	reproduced	28.75	46.32	24.74	43.98	30.04	51.20	27.84	47.16
	Paracosm	ours	37.14	56.23	31.93	54.19	40.29	62.37	36.45	57.60

trained generative model. Yet, they run along with other methods to warrant good CIR performance.

- *Training-free methods.* CIReVL [20] uses an LMM to generate a description of a given reference image, and then an LLM to modify this description based on the modification text. It uses the modified description for cross-modality retrieval in the image database. LDRE [57] proposes to generate multiple diverse descriptions to improve CIR performance. OSrCIR [44] carefully designs the prompt to an LMM with Reflective Chain-of-Thought to improve the output description quality for a multimodal query.

It is worth noting that, although the official papers of CIReVL [20] and OSrCIR [44] reported using CLIP [33] in experiments, their official open-source codes [1, 2] clarify or imply that their implementation actually uses OpenCLIP [18] on CIRCO, Fashion IQ, and GeneCIS. For fair and comprehensive comparisons, we re-implement OSrCIR using both CLIP and OpenCLIP VLMs, comparing using GPT-4o (used in its paper) and Qwen2.5-VL-7B-Instruct (used by our Paracosm) w.r.t description generation.

4.1. Benchmarking Results

Quantitative Results. Table 1, 2 and 3 display benchmarking results of all the compared methods, across different VLM backbones, with respect to different metrics on all the test sets. Convincingly, Paracosm resoundingly outperforms all the compared methods. Generally, with more powerful VLM models, e.g., ViT-L/14 > ViT-B/32, methods yield better CIR performance. Yet, it is worth noting that OSrCIR reported in its paper that it used CLIP for experiments on all datasets, but its open-source in Github [2] hints that it might have used OpenCLIP except on CIRCO. Therefore, we reimplement OSrCIR with both CLIP and OpenCLIP. Our reproduced results with OpenCLIP match what were reported in its paper. Moreover, with OSrCIR, we compare using GPT-4o and Qwen2.5-VL to generate descriptions, finding that the former yields better CIR results. Nevertheless, our Paracosm leverages the latter and still outperforms OSrCIR, which even exploits GPT-4o. Paracosm even rivals recent supervised learning CIR methods [13, 61].

Qualitative Results. Fig. 3 visually compares the retrieved images by Paracosm and the recent method OSr-

Table 3. Benchmarking results on the GeneCIS test set. GeneCIS has four subsets; we report the averaged numeric metrics for each method and provide detailed results in the supplementary Section F. Like in Table 1, we particularly study the recently published competitor OSrCIR with different backbones. We refer the reader to Table 1 caption for conclusions.

Backbone	Method	venue&year	R@1	R@2	R@3
CLIP ViT-B/32	Image-only	baseline	11.5	21.4	31.1
	Text-only	baseline	8.4	17.1	25.8
	Image+Text	baseline	12.7	23.7	32.9
	SEARLE [7]	ICCV'23	14.4	25.3	35.4
	CIREVL [20]	ICLR'24	15.9	26.8	36.8
	OSrCIR [44] w/ GPT-4o	CVPR'25	17.4	29.1	39.0
	OSrCIR w/ GPT-4o	reproduced	14.0	25.4	34.8
	OSrCIR w/ Qwen2.5-VL	reproduced	14.9	26.1	35.9
Paracosm		ours	16.1	26.3	36.3
CLIP ViT-L/14	Pic2Word [36]	CVPR'23	11.2	21.5	30.4
	SEARLE [7]	ICCV'23	12.3	22.1	31.3
	LinCIR [16]	CVPR'24	12.2	22.8	32.4
	CIG + LinCIR [52]	CVPR'25	12.5	22.7	32.3
	CIREVL [20]	ICLR'24	15.9	27.1	36.3
	OSrCIR [44] w/ GPT-4o	CVPR'25	17.9	29.0	38.7
	OSrCIR w/ GPT-4o	reproduced	14.4	25.0	34.9
	OSrCIR w/ Qwen2.5-VL	reproduced	15.0	26.4	36.3
Paracosm		ours	17.4	28.5	37.9
OpenCLIP ViT-B/32	OSrCIR w/ GPT-4o	reproduced	14.2	25.9	36.5
	OSrCIR w/ Qwen2.5-VL	reproduced	15.5	26.7	36.6
	Paracosm	ours	17.1	28.6	38.3
OpenCLIP ViT-L/14	OSrCIR w/ GPT-4o	reproduced	15.0	25.9	35.7
	OSrCIR w/ Qwen2.5-VL	reproduced	15.5	27.0	36.9
	Paracosm	ours	17.6	29.0	38.1

CIR [44], along with their generated mental images and descriptions, respectively. Clearly, generated descriptions by OSrCIR insufficiently represent given multimodal queries, whereas mental images by Paracosm preserve and capture rich visual details pertaining to the multimodal query. This helps explain why Paracosm outperforms OSrCIR.

4.2. Analyses and Ablation Study

λ for combining visual and textual features. Paracosm (Fig. 2) employs a hyperparameter λ (Eq. 1) to control the contribution of modification texts from the query. Fig. 4 studies its effects on the final CIR performance over the four benchmarks. Interestingly, $\lambda = 0.3$ consistently produces the highest numeric metrics on all the benchmarks. We set $\lambda = 0.3$ throughout our work.

Reference image editing vs. Text-to-Image generation. When generating mental images for multimodal queries, our Paracosm leverages the LMM to directly edit the reference images based on modification texts. In comparison, another workaround is T2I generation, as done in the recent work [26]: generating descriptions for reference images using an LMM, then modifying the descriptions based on modification texts using an LLM, and lastly generating mental images based on the modified descriptions. Table 4 compares them, clearly showing that Paracosm’s design choice leads to better performance.

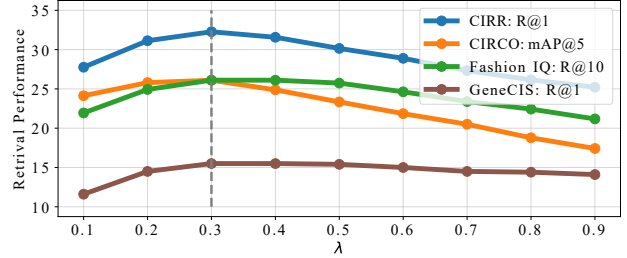


Figure 4. Analysis of λ which controls the importance of incorporating modification text in Eq. 1. Interestingly, on all datasets, setting $\lambda = 0.3$ consistently yields the highest numeric metrics reported for all the datasets.

Table 4. Comparing different generation methods for the mental images within Paracosm. Here, we adopt the CLIP ViT-B/32 VLM for Paracosm and report results on the CIRR test set. “T2I Generation” means first generating pseudo-target descriptions and then basing on them to generate mental images. “Image Edit” means our design choice for generating mental images in Paracosm, i.e., directly editing reference images based on modification texts. Clearly, the latter performs better.

Method	R@1	R@5	R@10	R@50
T2I Generation	31.71	61.37	73.59	91.54
Image Edit	32.27	62.60	75.16	92.60

Ablation Study. We ablate core components in Paracosm with the CLIP ViT-B/32 VLM on CIRR and CIRCO. Table 5 excerpts salient results; supplementary Section F provides comprehensive details.

- Incorporating mental images boosts performance.* While existing training-free methods generate descriptions t_{query} , aka pseudo-target descriptions [2], Paracosm further incorporates its generated mental images I_{mental} . This results in clearly performance gains.
- Incorporating synthetic counterparts of database images boosts performance.* As I_{mental} has synthetic-to-real domain gaps with database images, Paracosm further generates synthetic counterparts I_{syn}^i for them and uses such for matching (Eq. 1). Clearly, doing this significantly boosts the final performance.
- Incorporating modification texts boosts performance.* Intuitively, modification texts t_{mod} contain crucial keywords that can be leveraged for CIR. Indeed, results demonstrate that incorporating modification texts greatly boosts CIR performance further. This observation aligns with what are reported in prior works [7, 16, 52].

5. Impacts and Limitations

Societal Impacts. CIR is an important component of search services in many real-world applications such as e-commerce and fashion industry. The proposed Paracosm, by extensively leveraging LMMs, greatly advances the CIR area, as demonstrated by its strong performance on standard benchmark

Table 5. Ablation study. We ablate key components of Paracosm with the CLIP ViT-B/32 VLM on the CIRCO and CIRR test sets. Per Eq. 1, we focus on constructing features for *multimodal queries* and *database images*. \mathbf{I}_{mental} , \mathbf{t}_{query} , \mathbf{t}_{mod} indicate the generated mental image, description of the target image based on the query, and modification text, respectively. \mathbf{I}^i and \mathbf{I}_{syn}^i represent database images and their synthetic counterparts, respectively. Clearly, incorporating \mathbf{I}_{mental} , \mathbf{I}_{syn} , and \mathbf{t}_{mod} significantly boosts CIR performance.

multimodal query			database images		CIRR								CIRCO			
\mathbf{t}_{query}	\mathbf{I}_{mental}	\mathbf{t}_{mod}	\mathbf{I}^i	\mathbf{I}_{syn}^i	Recall@k				RecallSubset@k			mAP@k				
					k=1	k=5	k=10	k=50	k=1	k=2	k=3	k=5	k=10	k=25	k=50	
✓			✓		17.21	43.49	55.90	81.16	52.00	72.31	84.92	14.91	15.34	16.79	17.60	
✓	✓		✓		18.80	44.96	58.84	82.65	50.39	72.80	83.93	13.71	13.89	15.19	15.92	
✓	✓	✓	✓		27.93	57.11	70.29	90.31	61.88	80.70	90.70	18.29	18.69	20.45	21.27	
✓			✓	✓	22.46	50.99	63.59	84.58	53.88	74.80	86.27	16.72	17.41	19.19	20.11	
✓	✓		✓	✓	24.60	52.68	65.86	86.53	54.84	74.92	86.82	16.57	17.10	18.59	19.30	
✓	✓	✓	✓	✓	32.27	62.60	75.16	92.60	65.16	83.25	92.34	26.10	27.02	29.29	30.45	

datasets. It is worth noting that LMMs’ pretraining datasets might contain poisonous, offensive, and biased data, likely causing the LMMs to output inaccurate, biased and even harmful text descriptions and synthetic images. Moreover, Paracosm does not have an alerting mechanism for inappropriate multimodal queries, which may contain malicious modification texts or intend to retrieve inappropriate target images. If being forced to retrieve target images based on such queries, the intermediate mental images and retrieval outputs may lead to negative societal impacts.

Limitations and Future Work. Paracosm relies on the quality of LMM-generated mental images for the query and synthetic counterparts of database images, as well as text descriptions for them. This means that Paracosm’s performance is largely affected by their quality. These generated images might look visually plausible at first sight but often lack factual fidelity and fine-grained details. For instance, in the first row of Figure 5, the mental image contains a cartoon-style duck, which does not correspond to any actual items in real world and causes retrieval to fail. Future work can focus on improving methods for image generation or editing, and developing methods to handle erroneously generated visuals. Moreover, to achieve state-of-the-art performance, Paracosm uses slightly different prompt templates in the benchmarking datasets. This is largely because of ambiguous modification texts provided in the datasets, e.g., GeneCIS only provides names of objects to preserve in the multimodal query. Nevertheless, future work can develop methods that adopt LMMs to generate prompt templates adaptive to diverse types of multimodal queries for image generation.

6. Conclusions

We present Paracosm, a novel and rather simple training-free zero-shot CIR method. Different from most existing ZS-CIR methods, which rely on generated text descriptions of multimodal queries, Paracosm leverages LMMs to generate mental images for multimodal queries, offering rich visual information beneficial to CIR. Moreover, as the synthetic mental images have synthetic-to-real domain gaps with real



Figure 5. Failure cases. Paracosm can fail due to limitations of generative models, which can generate implausible and counterfactual mental images. Four examples in the four rows, respectively, demonstrate different failures of Paracosm. (1) It incorrectly generates a cartoon-style duck, making it fail to return the correct database image which captures a plush toy duck. (2) It generates a counterfactual oven which has gas burners on its door, making it incorrectly retrieve an image that captures a burning oven. (3) It fails to edit the door color of the specified refrigerator and hence fails to return the correct target image. (4) It fails to comprehend the multimodal query, resulting in an incorrect mental image and hence failing to return the correct target image.

database images, it further generates synthetic counterparts for database images. By incorporating the generated visuals as well as generated descriptions, it achieves state-of-the-art performance on four popular benchmarking datasets. Paracosm significantly outperforms existing ZS-CIR methods and even rivals supervised learning approaches.

References

[1] Github. https://github.com/ExplainableML/Vision_by_Language/issues/10. 2025.04.16. 6

[2] Github. <https://github.com/Pter61/osrcir/issues/5>. 2025.07.20. 5, 6, 7

[3] Lorenzo Agnolucci, Alberto Baldrati, Alberto Del Bimbo, and Marco Bertini. isearle: Improving textual inversion for zero-shot composed image retrieval. *IEEE Transactions on Pattern Analysis and Machine Intelligence (TPAMI)*, 47(11):10801–10817, 2025. 1, 4, 12

[4] Jinze Bai, Shuai Bai, Yunfei Chu, Zeyu Cui, Kai Dang, Xiaodong Deng, Yang Fan, Wenbin Ge, Yu Han, Fei Huang, et al. Qwen technical report. *arXiv preprint arXiv:2309.16609*, 2023. 2

[5] Shuai Bai, Keqin Chen, Xuejing Liu, Jialin Wang, Wenbin Ge, Sibo Song, Kai Dang, Peng Wang, Shijie Wang, Jun Tang, et al. Qwen2. 5-vl technical report. *arXiv preprint arXiv:2502.13923*, 2025. 2

[6] Alberto Baldrati, Marco Bertini, Tiberio Uricchio, and Alberto Del Bimbo. Effective conditioned and composed image retrieval combining clip-based features. In *Proceedings of the IEEE/CVF Conference on Computer Vision and Pattern Recognition (CVPR)*, pages 21466–21474, 2022. 1, 2, 5, 6

[7] Alberto Baldrati, Lorenzo Agnolucci, Marco Bertini, and Alberto Del Bimbo. Zero-shot composed image retrieval with textual inversion. In *Proceedings of the IEEE/CVF International Conference on Computer Vision (ICCV)*, pages 15338–15347, 2023. 1, 2, 3, 4, 5, 6, 7, 13, 15, 16

[8] Tong Bao, Che Liu, Derong Xu, Zhi Zheng, and Tong Xu. Milm-i2w: Harnessing multimodal large language model for zero-shot composed image retrieval. In *Proceedings of the 31st International Conference on Computational Linguistics (COLING)*, pages 1839–1849, 2025. 2

[9] Tim Brooks, Aleksander Holynski, and Alexei A. Efros. Instructpix2pix: Learning to follow image editing instructions. In *Proceedings of the IEEE/CVF Conference on Computer Vision and Pattern Recognition (CVPR)*, pages 18392–18402, 2023. 2

[10] Tom Brown, Benjamin Mann, Nick Ryder, Melanie Subbiah, Jared D Kaplan, Prafulla Dhariwal, Arvind Neelakantan, Pranav Shyam, Girish Sastry, Amanda Askell, et al. Language models are few-shot learners. *Advances in Neural Information Processing Systems (NeurIPS)*, 33:1877–1901, 2020. 1, 2

[11] Yanbei Chen and Loris Bazzani. Learning joint visual semantic matching embeddings for language-guided retrieval. In *European Conference on Computer Vision (ECCV)*, pages 136–152. Springer, 2020. 1, 2

[12] Yanbei Chen, Shaogang Gong, and Loris Bazzani. Image search with text feedback by visiolinguistic attention learning. In *Proceedings of the IEEE/CVF Conference on Computer Vision and Pattern Recognition (CVPR)*, pages 3001–3011, 2020. 1

[13] Yiyang Chen, Zhedong Zheng, Wei Ji, Leigang Qu, and Tat-Seng Chua. Composed image retrieval with text feedback via multi-grained uncertainty regularization. In *International Conference on Learning Representations (ICLR)*, 2024. 6

[14] Ginger Delmas, Rafael S Rezende, Gabriela Csurka, and Diane Larlus. Artemis: Attention-based retrieval with text-explicit matching and implicit similarity. In *International Conference on Learning Representations (ICLR)*, 2022. 1, 2

[15] Zhipeng Di, Guoxuan Zhu, Zhongjie Duan, Zihao Chu, Yingda Chen, and Weiyi Lu. Diffsynth-engine: a high-performance diffusion inference engine. <https://github.com/modelscope/diffsynth-engine>, 2025. 4

[16] Geonmo Gu, Sanghyuk Chun, Wonjae Kim, Yoohoon Kang, and Sangdoo Yun. Language-only training of zero-shot composed image retrieval. In *Proceedings of the IEEE/CVF Conference on Computer Vision and Pattern Recognition (CVPR)*, pages 13225–13234, 2024. 1, 2, 3, 4, 5, 6, 7, 15, 16

[17] Zhizhang Hu, Xinliang Zhu, Son Tran, René Vidal, and Arnab Dhua. Provla: Compositional image search with progressive vision-language alignment and multimodal fusion. In *Proceedings of the IEEE/CVF International Conference on Computer Vision (ICCV)*, pages 2772–2777, 2023. 2

[18] Gabriel Ilharco, Mitchell Wortsman, Ross Wightman, Cade Gordon, Nicholas Carlini, Rohan Taori, Achal Dave, Vaishaal Shankar, Hongseok Namkoong, John Miller, Hannaneh Hajishirzi, Ali Farhadi, and Ludwig Schmidt. Openclip, 2021. If you use this software, please cite it as below. 2, 6, 14

[19] Imagen-Team-Google. Imagen 3. *arXiv preprint arXiv:2408.07009*, 2024. 4

[20] Shyamgopal Karthik, Karsten Roth, Massimiliano Mancini, and Zeynep Akata. Vision-by-language for training-free compositional image retrieval. In *International Conference on Learning Representations (ICLR)*, 2024. 1, 2, 3, 4, 5, 6, 7, 13, 15, 16

[21] Seungmin Lee, Dongwan Kim, and Bohyung Han. Cosmo: Content-style modulation for image retrieval with text feedback. In *Proceedings of the IEEE/CVF Conference on Computer Vision and Pattern Recognition (CVPR)*, pages 802–812, 2021. 1, 2

[22] Matan Levy, Rami Ben-Ari, Nir Darshan, and Dani Lischinski. Data roaming and quality assessment for composed image retrieval. In *Proceedings of the AAAI Conference on Artificial Intelligence (AAAI)*, pages 2991–2999, 2024. 2

[23] Junnan Li, Dongxu Li, Caiming Xiong, and Steven Hoi. Blip: Bootstrapping language-image pre-training for unified vision-language understanding and generation. In *International Conference on Machine Learning (ICML)*, pages 12888–12900. PMLR, 2022. 2

[24] Mingyong Li, Zongwei Zhao, Xiaolong Jiang, and Zheng Jiang. Clip-probcr: Clip-based probability embedding combination retrieval. In *Proceedings of the 2024 International Conference on Multimedia Retrieval (ICMR)*, pages 1104–1109, 2024. 5

[25] Wei Li, Hehe Fan, Yongkang Wong, Yi Yang, and Mohan Kankanhalli. Improving context understanding in multimodal large language models via multimodal composition learning. In *Forty-first International Conference on Machine Learning (ICML)*, 2024. 2

[26] You Li, Fan Ma, and Yi Yang. Imagine and seek: Improving composed image retrieval with an imagined proxy. In *Proceedings of the IEEE/CVF Conference on Computer Vision*

and Pattern Recognition (CVPR), pages 3984–3993, 2025. 1, 2, 3, 4, 5, 7

[27] Tsung-Yi Lin, Michael Maire, Serge Belongie, James Hays, Pietro Perona, Deva Ramanan, Piotr Dollár, and C Lawrence Zitnick. Microsoft coco: Common objects in context. In *European Conference on Computer Vision (ECCV)*, pages 740–755. Springer, 2014. 12

[28] Yikun Liu, Jiangchao Yao, Ya Zhang, Yanfeng Wang, and Weidi Xie. Zero-shot composed text-image retrieval, 2024. 2

[29] Zheyuan Liu, Cristian Rodriguez-Opazo, Damien Teney, and Stephen Gould. Image retrieval on real-life images with pre-trained vision-and-language models. In *Proceedings of the IEEE/CVF International Conference on Computer Vision (ICCV)*, pages 2125–2134, 2021. 1, 4, 12

[30] Zheyuan Liu, Weixuan Sun, Yicong Hong, Damien Teney, and Stephen Gould. Bi-directional training for composed image retrieval via text prompt learning. In *Proceedings of the IEEE/CVF Winter Conference on Applications of Computer Vision (WACV)*, pages 5753–5762, 2024. 1, 2, 5

[31] Zheyuan Liu, Weixuan Sun, Damien Teney, and Stephen Gould. Candidate set re-ranking for composed image retrieval with dual multi-modal encoder. *Transactions on Machine Learning Research (TMLR)*, 2024. 2

[32] OpenAI. Gpt-4 technical report, 2024. 1, 2

[33] Alec Radford, Jong Wook Kim, Chris Hallacy, Aditya Ramesh, Gabriel Goh, Sandhini Agarwal, Girish Sastry, Amanda Askell, Pamela Mishkin, Jack Clark, et al. Learning transferable visual models from natural language supervision. In *International Conference on Machine Learning (ICML)*, pages 8748–8763. PMLR, 2021. 2, 6

[34] Robin Rombach, Andreas Blattmann, Dominik Lorenz, Patrick Esser, and Björn Ommer. High-resolution image synthesis with latent diffusion models. In *Proceedings of the IEEE/CVF Conference on Computer Vision and Pattern Recognition (CVPR)*, pages 10684–10695, 2022. 1, 2

[35] Olga Russakovsky, Jia Deng, Hao Su, Jonathan Krause, Sanjeev Satheesh, Sean Ma, Zhiheng Huang, Andrej Karpathy, Aditya Khosla, Michael Bernstein, Alexander C. Berg, and Li Fei-Fei. ImageNet Large Scale Visual Recognition Challenge. *International Journal of Computer Vision (IJCV)*, 115(3):211–252, 2015. 2, 3

[36] Kuniaki Saito, Kihyuk Sohn, Xiang Zhang, Chun-Liang Li, Chen-Yu Lee, Kate Saenko, and Tomas Pfister. Pic2word: Mapping pictures to words for zero-shot composed image retrieval. In *Proceedings of the IEEE/CVF Conference on Computer Vision and Pattern Recognition (CVPR)*, pages 19305–19314, 2023. 1, 2, 3, 4, 5, 6, 7, 13, 15, 16

[37] Axel Sauer, Dominik Lorenz, Andreas Blattmann, and Robin Rombach. Adversarial diffusion distillation. In *European Conference on Computer Vision (ECCV)*, pages 87–103. Springer, 2024. 1, 2

[38] Piyush Sharma, Nan Ding, Sebastian Goodman, and Radu Soricut. Conceptual captions: A cleaned, hypernymed, image alt-text dataset for automatic image captioning. In *Proceedings of the 56th Annual Meeting of the Association for Computational Linguistics (ACL)*, pages 2556–2565, 2018. 2, 3

[39] Xuemeng Song, Fuli Feng, Xianjing Han, Xin Yang, Wei Liu, and Liqiang Nie. Neural compatibility modeling with attentive knowledge distillation. In *The 41st International ACM SIGIR Conference on Research and Development in Information Retrieval (SIGIR)*, pages 5–14, 2018. 1

[40] Alane Suhr, Stephanie Zhou, Ally Zhang, Iris Zhang, Huajun Bai, and Yoav Artzi. A corpus for reasoning about natural language grounded in photographs. In *Proceedings of the 57th Annual Meeting of the Association for Computational Linguistics (ACL)*, pages 6418–6428, 2019. 12

[41] Hao Tan and Mohit Bansal. Lxmert: Learning cross-modality encoder representations from transformers. *arXiv preprint arXiv:1908.07490*, 2019. 2

[42] Yuanmin Tang, Jing Yu, Keke Gai, Jiamin Zhuang, Gang Xiong, Yue Hu, and Qi Wu. Context-i2w: Mapping images to context-dependent words for accurate zero-shot composed image retrieval. In *Proceedings of the AAAI Conference on Artificial Intelligence (AAAI)*, pages 5180–5188, 2024. 1, 2

[43] Yuanmin Tang, Jing Yu, Keke Gai, Jiamin Zhuang, Gang Xiong, Gaopeng Gou, and Qi Wu. Missing target-relevant information prediction with world model for accurate zero-shot composed image retrieval. In *Proceedings of the Computer Vision and Pattern Recognition Conference (CVPR)*, pages 24785–24795, 2025. 1, 2

[44] Yuanmin Tang, Jue Zhang, Xiaoting Qin, Jing Yu, Gaopeng Gou, Gang Xiong, Qingwei Lin, Saravan Rajmohan, Dongmei Zhang, and Qi Wu. Reason-before-retrieve: One-stage reflective chain-of-thoughts for training-free zero-shot composed image retrieval. In *Proceedings of the IEEE/CVF Conference on Computer Vision and Pattern Recognition (CVPR)*, pages 14400–14410, 2025. 1, 2, 3, 4, 5, 6, 7, 13, 15, 16

[45] Gemini Team. Gemini: a family of highly capable multimodal models. *arXiv preprint arXiv:2312.11805*, 2023. 2

[46] Qwen Team. Qwen2.5-vl, 2025. 3, 5, 12, 13

[47] Yuxin Tian, Shawn Newsam, and Kofi Boakye. Fashion image retrieval with text feedback by additive attention compositional learning. In *Proceedings of the Winter Conference on Applications of Computer Vision (WACV)*, pages 1011–1021, 2023. 2

[48] Hugo Touvron, Thibaut Lavril, Gautier Izacard, Xavier Martinet, Marie-Anne Lachaux, Timothée Lacroix, Baptiste Rozière, Naman Goyal, Eric Hambro, Faisal Azhar, Aurelien Rodriguez, Armand Joulin, Edouard Grave, and Guillaume Lample. Llama: Open and efficient foundation language models. *arXiv preprint arXiv:2302.13971*, 2023. 2

[49] Hugo Touvron, Louis Martin, Kevin Stone, Peter Albert, Amjad Almahairi, Yasmine Babaei, Nikolay Bashlykov, Soumya Batra, Prajjwal Bhargava, Shruti Bhosale, et al. Llama 2: Open foundation and fine-tuned chat models. *arXiv preprint arXiv:2307.09288*, 2023. 1

[50] Sagar Vaze, Nicolas Carion, and Ishan Misra. Genecis: A benchmark for general conditional image similarity. In *Proceedings of the IEEE/CVF Conference on Computer Vision and Pattern Recognition (CVPR)*, pages 6862–6872, 2023. 1, 4, 12

[51] Nam Vo, Lu Jiang, Chen Sun, Kevin Murphy, Li-Jia Li, Li Fei-Fei, and James Hays. Composing text and image for

image retrieval - an empirical odyssey. In *Proceedings of the IEEE/CVF Conference on Computer Vision and Pattern Recognition (CVPR)*, 2019. 1, 2

[52] Lan Wang, Wei Ao, Vishnu Naresh Boddeti, and Ser-Nam Lim. Generative zero-shot composed image retrieval. In *Proceedings of the IEEE/CVF Conference on Computer Vision and Pattern Recognition (CVPR)*, pages 29690–29700, 2025. 1, 2, 3, 4, 5, 6, 7, 15, 16

[53] Chenfei Wu, Jiahao Li, Jingren Zhou, Junyang Lin, Kaiyuan Gao, Kun Yan, Sheng ming Yin, Shuai Bai, Xiao Xu, Yilei Chen, Yuxiang Chen, Zecheng Tang, Zekai Zhang, Zhengyi Wang, An Yang, Bowen Yu, Chen Cheng, Dayiheng Liu, Deqing Li, Hang Zhang, Hao Meng, Hu Wei, Jingyuan Ni, Kai Chen, Kuan Cao, Liang Peng, Lin Qu, Minggang Wu, Peng Wang, Shuting Yu, Tingkun Wen, Wensen Feng, Xiaoxiao Xu, Yi Wang, Yichang Zhang, Yongqiang Zhu, Yujia Wu, Yuxuan Cai, and Zenan Liu. Qwen-image technical report, 2025. 2, 3, 5, 12, 13

[54] Hui Wu, Yupeng Gao, Xiaoxiao Guo, Ziad Al-Halah, Steven Rennie, Kristen Grauman, and Rogerio Feris. Fashion iq: A new dataset towards retrieving images by natural language feedback. In *Proceedings of the IEEE/CVF Conference on Computer Vision and Pattern Recognition (CVPR)*, pages 11307–11317, 2021. 1, 4, 12

[55] Yahui Xu, Yi Bin, Jiwei Wei, Yang Yang, Guoqing Wang, and Heng Tao Shen. Multi-modal transformer with global-local alignment for composed query image retrieval. *IEEE Transactions on Multimedia (TMM)*, 25:8346–8357, 2023. 2

[56] Yuchen Yang, Yu Wang, and Yanfeng Wang. Sda: Semantic discrepancy alignment for text-conditioned image retrieval. In *Findings of the Association for Computational Linguistics (ACL)*, pages 5250–5261, 2024. 2

[57] Zhenyu Yang, Dizhan Xue, Shengsheng Qian, Weiming Dong, and Changsheng Xu. Ldre: Llm-based divergent reasoning and ensemble for zero-shot composed image retrieval. In *Proceedings of the 47th International ACM SIGIR Conference on Research and Development in Information Retrieval (SIGIR)*, pages 80–90, 2024. 1, 2, 3, 4, 5, 6, 16

[58] Tianwei Yin, Michaël Gharbi, Richard Zhang, Eli Shechtman, Fredo Durand, William T Freeman, and Taesung Park. One-step diffusion with distribution matching distillation. In *Proceedings of the IEEE/CVF Conference on Computer Vision and Pattern Recognition (CVPR)*, pages 6613–6623, 2024. 4

[59] Kai Zhang, Yi Luan, Hexiang Hu, Kenton Lee, Siyuan Qiao, Wenhui Chen, Yu Su, and Ming-Wei Chang. MagicLens: Self-supervised image retrieval with open-ended instructions. In *International Conference on Machine Learning (ICML)*, pages 59403–59420. PMLR, 2024. 1, 2

[60] Xu Zhang, Zhedong Zheng, Linchao Zhu, and Yi Yang. Collaborative group: Composed image retrieval via consensus learning from noisy annotations. *Knowledge-Based Systems (KBS)*, 300:112135, 2024. 2

[61] Yida Zhao, Yuqing Song, and Qin Jin. Progressive learning for image retrieval with hybrid-modality queries. In *Proceedings of the 45th international ACM SIGIR Conference on Research and Development in Information Retrieval (SIGIR)*, pages 1012–1021, 2022. 2, 6

[62] Dewei Zhou, You Li, Fan Ma, Xiaoting Zhang, and Yi Yang. Mige: Multi-instance generation controller for text-to-image synthesis. In *Proceedings of the IEEE/CVF Conference on Computer Vision and Pattern Recognition (CVPR)*, pages 6818–6828, 2024. 1, 2, 4

Generating a Paracosm for Training-Free Zero-Shot Composed Image Retrieval

Supplementary Material

This document supports our main paper with detailed results and comprehensive analyses. Here is the outline of the document:

- **Section A** shows additional details of benchmark datasets.
- **Section B** describes detailed prompts for image generation.
- **Section C** contains the qualitative analysis of mental images for queries and synthetic counterparts for database images.
- **Section D** presents further analyses of LMMs in Paracosm.
- **Section E** introduces the demo code as part of the supplementary material.
- **Section F** provides detailed quantitative results for each dataset.

A. Additional Details of Benchmark Datasets

In this section, we provide additional details of four benchmark datasets, i.e., CIRR [29], CIRCO [3], Fashion IQ [54], and GeneCIS [50]. In addition, we summarize the datasets used in our experiments in Table 6.

- Compose Image Retrieval on Real-life images (CIRR) dataset collects negative images with high visual similarity from NLVR² [40]. To mitigate the false negative issue, CIRR clusters visually similar images into subsets. Since each subset contains images similar to the target image, evaluating retrieval within this constrained subset places greater demands on the model’s discriminative capability.
- Composed Image Retrieval on Common Objects in context (CIRCO) is based on open-domain real-world images [27]. It is the first dataset for CIR with multiple ground truths and fine-grained semantic annotations.
- Fashion Interactive Queries (Fashion IQ) contains diverse fashion images (dresses, shirts, and tops&tees) from Amazon.com. While it is a challenging dataset, the test set is not publicly accessible.
- General Conditional Image Similarity (GeneCIS) is designed for zero-shot evaluation only, which includes four subsets: Focus Attribute, Change Attribute, Focus Object, and Change Object, representing four different tasks. To reduce the impact of false negatives, a gallery is selected for each query, which serves as the database, with gallery sizes ranging from 10 to 15 images. Unlike other datasets, which provide modification texts, GeneCIS only provides a single object name or attribute as the retrieval condition.

B. Detailed Prompts for Generation.

In our work, we leverage large multimodal models (LMMs) [46, 53] to generate mental images, synthetic coun-

Table 6. Statistics of datasets for ZS-CIR. We list the numbers of queries in the test set and the numbers of candidate images in the database for each dataset. Since our Paracosm is a training-free ZS-CIR method, we only list the test or validation sets (as Fashion IQ only releases its validation set) used in our experiments. Notably, for GeneCIS, to reduce the impact of false negatives, a gallery is selected for each query to serve as the database, with gallery sizes ranging from 10 to 15 images.

Dataset	subset	# queries	# database images
CIRR [29]	–	4,148	2,315
CIRCO [3]	–	800	123,403
Fashion IQ [54]	Shirt	2,038	6,346
	Dress	2,017	3,817
	Toptee	1,961	5,373
GeneCIS [50]	Focus Attribute	2,000	10
	Change Attribute	2,112	15
	Focus Object	1,960	15
	Change Object	1,960	15

terparts, and their textual descriptions. Taking into account the differences in modification texts across datasets, we employ dataset-specific prompting strategies to generate mental images. In Figures 6 and 7, we show the prompt templates that are used to generate mental images for different datasets. Prompt templates for generating textual descriptions of candidate images and mental images are shown in Figure 8. The detailed textual descriptions of candidate images are then used as prompts for text-to-image (T2I) generation of synthetic counterparts. For all image generation tasks, we set the output image size to 512×512 . All other generation parameters are retained at their default values, as recommended by the official implementation. We also provide detailed generation processes in our demo file (demo.ipynb).

C. Qualitative Analysis of Mental and Synthetic Counterparts

To gain deeper insight into the behavior of our Paracosm, we visualize the generated mental images and synthetic counterparts across datasets. As shown in Fig. 10, we leverage Qwen-Image-Edit [53] to modify the reference image into a mental image, conditioned on the provided modification text. For the Genesis dataset, where modification texts are single words or short phrases (e.g., “color”, “donut”), we apply carefully designed prompt templates (detailed in Fig. 7) to ensure that even a single word is effectively interpreted as a meaningful visual modification. As the generated mental image has synthetic-to-real domain gaps from the real images in the dataset, we generate a synthetic counterpart for each candidate image based on its detailed textual description.

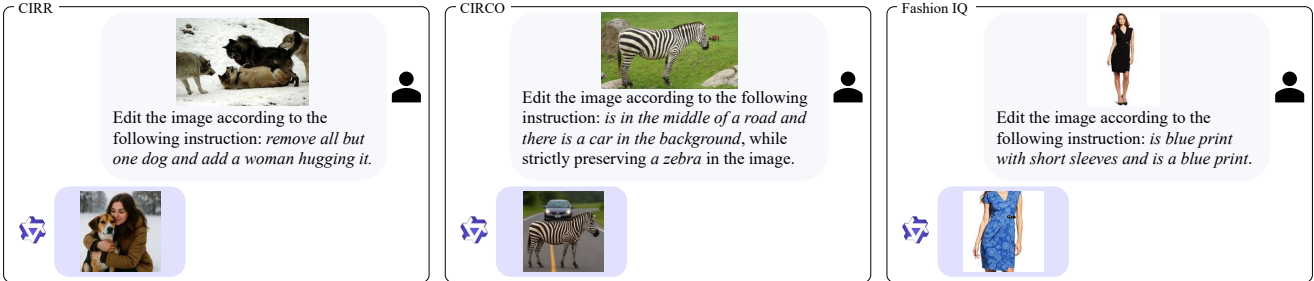


Figure 6. **Prompt templates used for mental image generation on CIRR, CIRCO, and Fashion IQ.** The italicized text in the figure corresponds to the modification text provided in each dataset. Notably, for the CIRCO dataset, both the modification text and the shared concept are available. So we incorporate the shared concept for better mental image generation. For all datasets, we use Qwen-Image-Edit [53] LMM through its editing mode to generate mental images. We also provide the demo file (demo.ipynb) that shows detailed process for mental image generation.

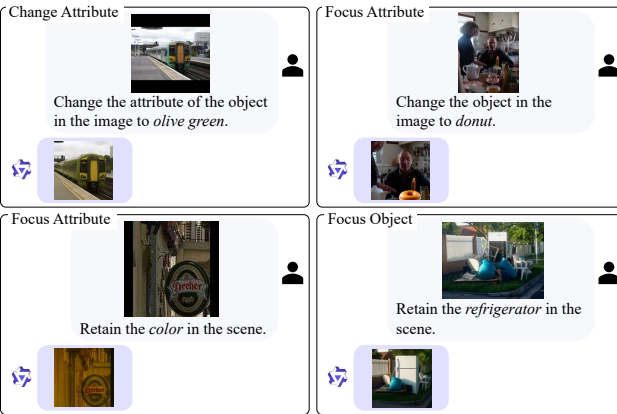


Figure 7. **Prompt templates used for mental image generation on GeneCIS.** Since the modification texts in GeneCIS are single words or short phrases (e.g., “color”, “donut”), we expand them into more descriptive instructions to ensure effective visual editing. As illustrated in the figure, we employ task-specific prompting strategies. For “Focus” tasks, we use the template “Retain the *modification text* in the scene.”. For “Change Attribute” task, the prompt template is “Change the attribute of the object in the image to *modification text*”. For “Change Object” task, we use “Change the object in the image to *modification text*”. The italicized text in the figure corresponds to the modification text provided in each subset. To generate mental images, we use Qwen-Image-Edit [53] LMM through its editing mode.

These synthetic counterparts are generated to preserve fine-grained visual attributes of the original candidate images and to mitigate synthetic-to-real domain gaps.

D. Further Analyses of LMMs

We further analyze the impact of using different LMMs for generating textual descriptions of mental images. Specifically, we replace Qwen2.5-VL-7B-Instruct [46] used in Paracosm with GPT-4o, the LMM employed by OSrCIR [44]. As shown in Tab. 8, switching to GPT-4o yields only marginal improvements in retrieval performance. Notably, the best performance across all datasets is achieved when $\lambda = 0.3$

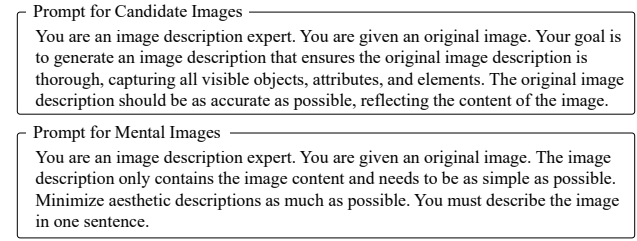


Figure 8. **Prompt templates for generating descriptions of candidate images (top) and mental images (bottom).** As illustrated in Figure 2, the detailed generated descriptions of candidate images are then used as prompts to generate synthetic counterparts. In contrast, the descriptions of mental images are intentionally constrained to a single sentence.

Table 7. **Detailed results on four datasets for Fig. 1.** The results in this table are obtained using the OpenCLIP ViT-G/14 backbone, enabling a fair comparison across methods. We report quantitative results for methods on CIRR, CIRCO, Fashion IQ, and GeneCIS, corresponding to the visual comparison presented in Fig. 1. For FashionIQ, we break down results by subset: “Shirt”, “Dress”, and “Toptee”. For GeneCIS, the subsets “FA”, “CA”, “FO”, and “CO” denote “Focus Attribute”, “Change Attribute”, “Focus Object”, and “Change Object”, respectively. * denotes the results obtained from reproduction.

	Pic2Word [36]	SEARLE [7]	CIReVL [20]	OSrCIR* [44]	Paracosm
CIRR (R@1)	30.41	34.80	34.65	37.59	39.30
CIRCO (mAP@5)	5.54	13.20	26.77	25.62	39.82
Shirt (R@10)	33.17	36.46	33.71	35.67	40.48
Dress (R@10)	25.43	28.16	27.07	29.80	33.17
Toptee (R@10)	35.24	39.83	35.80	36.51	42.58
FA (R@1)	12.50	16.30	20.50	19.10	21.40
CA (R@1)	11.70	16.20	16.10	13.20	16.90
FO (R@1)	9.90	10.80	14.70	13.50	18.20
CO (R@1)	8.60	8.30	18.10	12.80	20.80

(Fig. 4), indicating that the final retrieval performance is relatively insensitive to the choice of LMM for mental image description generation. This indicates that the core strength of Paracosm lies not in the scale of LMMs but in the “paracosm” constructed by our method. Additionally, we generate brief textual descriptions (\mathbf{t}_{brief}^i) for candidate images and

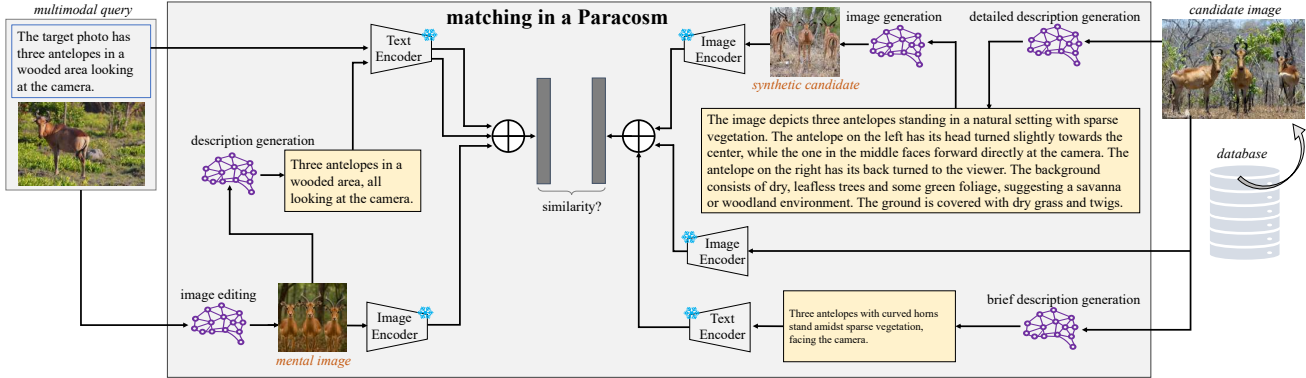


Figure 9. **Extended flowchart of Paracosm incorporating brief candidate image descriptions (w/ t_{brief}^i).** This variant introduces an additional branch that generates and integrates brief candidate image descriptions (w/ t_{brief}^i) into Paracosm. This version supports the study in Sec. D evaluating the impact of brief candidate image descriptions on performance.

Table 8. Further analyses. We evaluate two potential enhancements to Paracosm: replacing Qwen2.5-VL with GPT-4o for generating mental image descriptions and incorporating brief candidate image descriptions (w/ t_{brief}^i) into the pipeline (see overview in Fig. 9). However, neither change leads to significant performance gains. These results indicate that our Paracosm is already well-optimized, with limited room for improvement from using larger LMMs or augmenting candidate descriptions.

Method	CIRR		CIRCO		Fashion IQ		GeneCIS	
	Recall@k k=1	k=50	mAP@k k=5	k=50	R@10	R@50	R@1	R@3
w/ GPT4o	31.86	92.41	26.44	30.85	26.65	46.14	14.7	34.2
w/ Qwen2.5-VL	32.27	92.60	26.10	30.45	26.14	46.39	16.1	36.3
w/ t_{brief}^i	32.89	92.82	26.95	31.20	26.06	45.56	11.9	31.7

incorporate them into Paracosm, as illustrated in Fig. 9. However, as shown in Tab. 8, this strategy yields performance gains only on the CIRR and CIRCO datasets. Consequently, we opt to exclude t_{brief}^i from our final pipeline.

E. Open-Source Code

We provide comprehensive demo code (`demo.ipynb`) in the Supplementary Material to enhance reproducibility and accessibility. The demo file showcases the complete implementation of Paracosm. It includes the processes of mental image generation, description generation, and synthetic counterpart generation. Additionally, we present the retrieval process of Paracosm on the CIRCO validation set. We also provide `README.md` with detailed guidelines on how to set up the environment and run the demo of Paracosm.

F. Detailed Quantitative Results

We provide additional results in this section to further support the findings presented in the main paper. We include detailed numerical values corresponding to the radar plot (Fig. 1) in Tab. 7, offering a quantitative basis for comparing different methods across datasets. Secondly, we provide

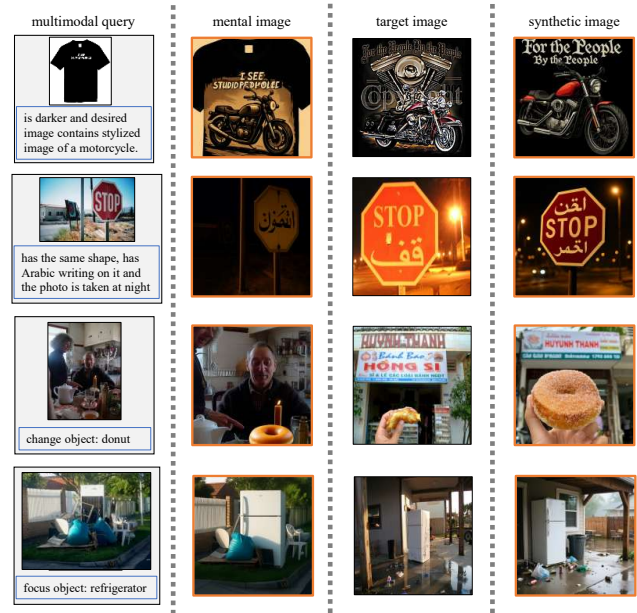


Figure 10. **More examples related to Paracosm.** The first column presents the reference image paired with its corresponding modification text. The second column displays the mental images based on the queries. The third column shows the ground-truth target images. The fourth column contains the synthetic counterparts generated from the detailed textual descriptions of the target images.

detailed results for each subset on GeneCIS in Tab. 9, supporting the averaged results in Tab. 3. In addition to the ablation study shown in Tab. 5, we extend the analysis with two additional variants: using only synthetic counterparts without candidate images and adding detailed descriptions of candidate images in Tab. 10. Tabs. 11 to 13 report benchmarking results on datasets using OpenCLIP ViT-G/14 [18] as the backbone. Under this unified setting, our method achieves the best or second-best performance on all datasets.

Table 9. **Detailed results on the GeneCIS test set.** We report detailed results for each subset of GeneCIS, complementing the averaged results presented in Tab. 3. Like in Tab. 1, we particularly study the recently published competitor OSrCIR with different backbones. Refer to Tab. 1 caption for conclusions.

Backbone	Method	venue&year	Focus Attribute			Change Attribute			Focus Object			Change Object		
			R@1	R@2	R@3	R@1	R@2	R@3	R@1	R@2	R@3	R@1	R@2	R@3
CLIP ViT-B/32	Image-only	baseline	18.1	29.6	40.4	9.7	19.6	29.9	9.7	18.9	27.2	8.6	17.6	26.7
	Text-only	baseline	10.6	21.1	30.3	10.2	16.9	24.4	5.7	14.6	23.7	7.2	15.8	24.8
	Image+Text	baseline	17.5	29.7	39.5	11.2	21.9	30.3	11.8	21.9	31.8	10.4	21.3	29.9
	SEARLE [7]	ICCV'23	18.9	30.6	41.2	13.0	23.8	33.7	12.2	23.0	33.3	13.6	23.8	33.3
	CIReVL [20]	ICLR'24	17.9	29.4	40.4	14.8	25.8	35.8	14.6	24.3	33.3	16.1	27.8	37.6
	OSrCIR [44] w/ GPT4o	CVPR'25	19.4	32.7	42.8	16.4	27.7	38.1	15.7	25.7	35.8	18.2	30.1	39.4
	OSrCIR w/ GPT4o	reproduced	16.2	30.7	41.2	13.0	23.3	32.2	13.2	23.7	32.5	13.5	23.9	33.2
	OSrCIR w/ Qwen2.5-VL	reproduced	18.1	30.8	41.6	13.4	24.7	33.8	15.4	26.1	34.5	12.9	23.0	33.7
CLIP ViT-L/14	Paracosm	ours	19.0	29.7	40.9	14.3	23.5	33.4	15.6	24.5	34.1	15.6	27.4	37.0
	Pic2Word [36]	CVPR'23	15.7	28.2	38.7	13.9	24.7	33.1	8.4	18.0	25.8	6.7	15.1	24.0
	SEARLE [7]	ICCV'23	17.0	29.7	40.7	16.4	25.3	34.1	7.8	16.7	25.3	7.9	16.8	25.1
	LinCIR [16]	CVPR'24	16.9	30.0	41.5	16.2	28.0	36.8	8.3	17.4	26.2	7.4	15.7	25.0
	CIG + LinCIR [52]	CVPR'25	17.0	29.4	40.4	16.1	28.6	37.2	8.4	17.5	26.7	8.6	15.4	24.9
	CIReVL [20]	ICLR'24	19.5	31.8	42.0	14.4	26.0	35.2	12.3	21.8	30.5	17.2	28.9	37.6
	OSrCIR [44] w/ GPT4o	CVPR'25	20.9	33.1	44.5	17.2	28.5	37.9	15.0	23.6	34.2	18.4	30.6	38.3
	OSrCIR w/ GPT4o	reproduced	18.3	29.3	39.8	13.3	24.1	31.7	13.0	23.4	34.5	13.2	23.2	33.8
OpenCLIP ViT-B/32	OSrCIR w/ Qwen2.5-VL	reproduced	19.4	30.2	41.4	13.8	24.8	33.0	13.8	24.9	34.8	13.2	25.5	36.0
	Paracosm	ours	20.8	32.7	41.5	14.6	23.6	33.6	17.0	28.7	38.3	17.2	28.9	38.4
	OSrCIR w/ GPT4o	reproduced	17.8	31.7	43.6	11.8	22.8	32.6	13.9	24.4	34.9	13.5	24.6	35.2
	OSrCIR w/ Qwen2.5-VL	reproduced	20.1	32.6	43.4	12.7	23.6	33.7	15.5	25.7	34.0	13.7	24.9	35.4
OpenCLIP ViT-L/14	Paracosm	ours	20.1	31.2	42.3	14.8	26.3	35.5	16.4	27.0	36.0	17.2	29.9	39.5

Table 10. **Ablation study.** The results in this table are obtained on CLIP ViT-B/32. To evaluate the role of each component in our framework, we conduct a comprehensive ablation study by removing one module at a time while keeping the rest unchanged. based on candidate images. The red part in the table means images and texts from multimodal queries or generated based on multimodal queries. The blue part means images and texts from database or generated based on candidate images. (\mathbf{I}_{mental} , \mathbf{t}_{query} , \mathbf{t}_{mod}) means (mental image, corresponding text description, modification text). (\mathbf{I}^i , \mathbf{I}_{syn}^i , $\mathbf{t}_{detailed}^i$) means (candidate image, synthetic counterpart, detailed description of candidate image). Paracosm's results are highlighted in bold.

multimodal query features			candidate features			CIRR						CIRCO				
\mathbf{I}_{mental}	\mathbf{t}_{query}	\mathbf{t}_{mod}	\mathbf{I}^i	\mathbf{I}_{syn}^i	$\mathbf{t}_{detailed}^i$	Recall@k			Recall _{Subset} @k			mAP@k				
						k=1	k=5	k=10	k=50	k=1	k=2	k=3	k=5	k=10	k=25	k=50
✓	✓	✓	✓	✓	✓	15.35	38.34	51.66	75.35	45.42	67.59	81.52	8.42	8.52	9.50	10.01
						17.21	43.49	55.90	81.16	52.00	72.31	84.92	14.91	15.34	16.79	17.60
	✓	✓	✓	✓	✓	18.80	44.96	58.84	82.65	50.39	72.80	83.93	13.71	13.89	15.19	15.92
	✓	✓	✓	✓	✓	27.93	57.11	70.29	90.31	61.88	80.70	90.70	18.29	18.69	20.45	21.27
✓	✓	✓	✓	✓	✓	17.64	41.93	54.46	77.37	48.36	69.11	83.21	10.06	10.43	11.44	12.03
						17.21	43.93	56.29	80.10	50.94	71.81	84.53	13.58	13.92	15.44	16.30
	✓	✓	✓	✓	✓	19.95	46.29	59.98	82.34	51.42	72.17	84.80	14.07	14.43	15.76	16.42
	✓	✓	✓	✓	✓	25.95	54.24	67.16	88.84	60.80	79.71	89.74	17.43	17.98	19.62	20.46
✓	✓	✓	✓	✓	✓	20.82	48.48	60.68	82.72	51.33	72.24	84.94	13.48	13.79	15.24	15.89
						22.46	50.99	63.59	84.58	53.88	74.80	86.27	16.72	17.41	19.19	20.11
	✓	✓	✓	✓	✓	24.60	52.68	65.86	86.53	54.84	74.92	86.82	16.57	17.10	18.59	19.30
	✓	✓	✓	✓	✓	32.27	62.60	75.16	92.60	65.16	83.25	92.34	26.10	27.02	29.29	30.45
✓	✓	✓	✓	✓	✓	22.31	50.94	63.86	85.01	52.96	73.71	85.98	13.88	14.48	15.87	16.57
						22.19	50.02	62.36	84.43	53.37	75.64	86.60	13.66	14.32	15.81	16.57
	✓	✓	✓	✓	✓	25.33	54.94	67.37	87.59	56.77	76.43	87.71	19.93	20.52	22.23	23.11
	✓	✓	✓	✓	✓	28.33	57.30	70.39	90.89	62.39	81.01	91.35	21.05	21.53	23.48	24.46

Table 11. **Benchmarking results on CIRCO and CIRR test sets.** Our Paracosm resoundingly outperforms all the compared methods on the two benchmarks. Refer to Tab. 1 caption for conclusions.

Backbone	Method	venue&year	CIRR						CIRCO				
			Recall@k			Recall _{Subset} @k			mAP@k				
			k=1	k=5	k=10	k=1	k=2	k=3	k=5	k=10	k=25	k=50	
OpenCLIP ViT-G/14	Pic2Word [36]	CVPR'23	30.41	58.12	69.23	68.92	85.45	93.04	5.54	5.59	6.68	7.12	
	SEARLE [7]	ICCV'23	34.80	64.07	75.11	68.72	84.70	93.23	13.20	13.85	15.32	16.04	
	LinCIR [16]	CVPR'24	35.25	64.72	76.05	63.35	82.22	91.98	19.71	21.01	23.13	24.18	
	CIG + LinCIR [52]	CVPR'25	36.05	66.31	76.96	64.94	83.18	91.93	20.64	21.90	24.04	25.20	
	LDRE [57]	SIGIR'24	36.15	66.39	77.25	68.82	85.66	93.76	31.12	32.24	34.95	36.03	
	CIReVL [20]	ICLR'24	34.65	64.29	75.06	67.95	84.87	93.21	26.77	27.59	29.96	31.03	
	OSrCIR [44] w/ GPT-4o	CVPR'25	37.26	67.25	77.33	69.22	85.28	93.55	30.47	31.14	35.03	36.59	
	OSrCIR w/ GPT-4o	reproduced	37.59	66.99	78.15	69.54	86.31	93.78	25.62	27.18	29.66	30.73	
Paracosm		ours	39.30	70.41	80.39	70.82	86.92	94.46	39.82	40.86	43.96	45.05	

Table 12. **Benchmarking results on the Fashion IQ validation set.** Paracosm performs the best or second best on OpenCLIP ViT-G/14. Like in Table 1, we particularly study the recently published competitor OSrCIR. Refer to Table 1 caption for conclusions.

Backbone	Method	venue&year	Shirt		Dress		Toptee		Average	
			R@10	R@50	R@10	R@50	R@10	R@50	R@10	R@50
OpenCLIP ViT-G/14	Pic2Word [36]	CVPR'23	33.17	50.39	25.43	47.65	35.24	57.62	31.28	51.89
	SEARLE [7]	ICCV'23	36.46	55.35	28.16	50.32	39.83	61.45	34.82	55.71
	LinCIR [16]	CVPR'24	46.76	65.11	38.08	60.88	50.48	71.09	45.11	65.69
	LDRE [57]	SIGIR'24	35.94	58.58	26.11	51.12	35.42	56.67	32.49	55.46
	CIReVL [20]	ICLR'24	33.71	51.42	27.07	49.53	35.80	56.14	32.19	52.36
	OSrCIR [44] w/ GPT-4o	CVPR'25	38.65	54.71	33.02	54.78	41.04	61.83	37.57	57.11
	OSrCIR w/ GPT-4o	reproduced	35.67	54.81	29.80	52.90	36.51	58.80	33.99	55.50
	Paracosm	ours	40.48	57.80	33.17	55.18	42.58	64.20	38.74	59.06

Table 13. **Benchmarking results on the GeneCIS test set.** Paracosm performs the best or second best on OpenCLIP ViT-G/14. Like in Table 1, we particularly study the recently published competitor OSrCIR. We refer the reader to Table 1 caption for conclusions.

Backbone	Method	venue&year	Focus Attribute			Change Attribute			Focus Object			Change Object		
			R@1	R@2	R@3	R@1	R@2	R@3	R@1	R@2	R@3	R@1	R@2	R@3
OpenCLIP ViT-G/14	Pic2Word [36]	CVPR'23	12.5	23.4	33.7	11.7	21.9	30.9	9.9	19.3	27.4	8.6	18.2	26.1
	SEARLE [7]	ICCV'23	16.3	29.4	40.7	16.2	27.3	35.5	10.8	18.2	27.9	8.3	15.6	25.8
	CIReVL [20]	ICLR'24	20.5	34.0	44.5	16.1	28.6	39.4	14.7	25.2	33.0	18.1	31.2	41.0
	OSrCIR [44] w/ GPT4o	CVPR'25	22.7	36.4	47.0	17.9	30.8	42.0	16.9	28.4	36.7	21.0	33.4	44.2
	OSrCIR w/ GPT4o	reproduced	19.1	30.4	41.3	13.2	23.3	32.9	13.5	23.9	32.7	12.8	24.8	34.5
	Paracosm	ours	21.4	34.5	45.8	16.9	26.8	36.3	18.2	29.3	37.5	20.8	32.2	41.5